International Journal of Engineering and Geosciences
https://dergipark.org.tr/en/pub/ijeg
e-ISSN 2548-0960

Registration of interferometric DEM by deep artificial neural networks using GPS control points coordinates as network target

Ahmed Serwa[*1], **Abdul Baser Qasimi** [2], **Vahid Isazade** [3]

[1] *Helwan University, Department of Civil Engineering, Cairo, Egypt, ahmed_serwa@yahoo.com*
[2] *Samangan University, Department of Geography, Samangan, Afghanistan, qasimi.abdul.a@smgu.edu.af*
[3] *Kharazmi University, Department of Geographical Sciences, Tehran, Iran, vahidisazade75@gmail.com*

Cite this study: Serwa, A., Qasimi, A. B., & Isazade, V. (2024). Registration of interferometric DEM by deep artificial neural networks using GPS control points coordinates as network target. International Journal of Engineering and Geosciences, 9 (2), 292-301

https://doi.org/10.26833/ijeg.1467293

Keywords
Remote sensing
DEM
Registration
Distortion

Research Article

Received: 09.04.2024
Revised: 05.05.2024
Accepted: 06.05.2024
Published:25.07.2024

Abstract

The interferometric Shuttle Radar Topography Mission (SRTM) satellite's digital elevation model (DEM) is an important tool for studying topographic features on a medium-spacing scale. Data were collected and processed using the satellite's orbital and navigation parameters with selected global GPS stations for verification. Distortion may be expressed by surveying measurements, such as position, distance, area, and shape. This study focuses on this distortion and proposes a new registration method to reduce its effect. Because of generality, the purpose shapes were excluded from this study. The proposed registration method depends on precise GPS control points that act as the ground truth for describing the considered surveying measurements. The processing was carried out using deep artificial neural networks (DANN) to produce a new registered DEM. A comparison was made between the original DEM and the new one, focusing on the selected surveying measurements. Another comparison was made between the GPS coordinates and SRTM polynomials to determine the potential of the proposed system. Some statistical investigations were applied to determine the level of significance of the distortion in each surveying measurement. The study shows that the distortion is highly significant; therefore, the proposed registration method is recommended to fix the distortion. An important finding is the enhancement in local coordinates scope.

1. Introduction

Remote sensing is a technology used to reduce costs and time by adopting automation [1]. The Radar Shuttle Radar Topography Mission (SRTM) collects interferometric radar data to produce near-global topographic products [2]. SRTM data are the main source of global topographic data, which depend on orbital navigation parameters to compute the space coordinates of the ground surface in addition to predefined ground control points (GCPs) for verification. The accuracy of the SRTM data varies from place to place, owing to the difference between the system reference properties and the proposed local reference properties. The accuracy of the SRTM DEM has been thoroughly investigated allover of the world in many countries [3]. Many trials have been conducted to achieve the best performance of the SRTM DEM for use in engineering applications, for example, not for exclusion of the following research works. Su and Guo [4] developed a practical way to correct the SRTM DEM in vegetated areas based on light detection and ranging (LiDAR) data. A similar investigation was conducted by Su et al. [5] but optical satellite images were added as a source for validation. Ochoa et al. [6] developed a methodology for the correction of digital elevation models for plain topography based on ground control points using a traditional methodology. Zhou et al. [7] investigated an adaptive terrain-dependent methodology for SRTM DEM correction for hard topography based on the M-estimator. Julzarika, Harintaka and Kartika [8] fused multiple DEM data sources, including SRTM DEM, to reach the optimum representation of vegetation areas. The use of artificial intelligence (AI) in remote sensing is an important modern aspect [9]. Deep artificial neural networks (DANN) provide good results in the processing and optimization of remote sensing data [10]. In addition to the previous literature, some research handle DEM from

different point of view, such as: Altunel [11] who studied the effect of DEM resolution on topographic wetness index. Bildirici and Abbak [12] studied the accuracy of SRTM DEM in comparison to local data within Turkey. Çubukçu et. al., [13] studied digital elevation modeling using artificial neural networks from the side of deterministic and geostatistical interpolation methods. Yakar [14] who studied Digital elevation model generation using robotic total station. Yalçın [15] studied DEM and GIS-based assessment of structural elements in the collision zone with a case study. Yılmaz and Erdogan [16] studied Designing high resolution countrywide DEM for Turkey. Yakar [17] investigated the effect of the grid resolution on the description of the surface. While Sarıturk [18] study on object detection and classification are among the most popular topics in Photogrammetry and Remote Sensing studies. Yakar et. al., [19] studied the performance of photogrammetric and terrestrial laser scanning methods in volume computing of excavation and filling sites. non-invasive, and inexpensive data collection technique [20] Yılmaz studied on examination the role of erosion of the surrounding soil by using Digital Elevation Model (DEM) [21].

This study attempts to find a practical approach to refine and register the SRTM DEM to the global reference to produce a corrected local one. To accomplish this research objective, one must understand the source of the SRTM DEM error. The error sources may vary in effect and value; therefore, we mention only the most effective and sensible sources according to the common literature. “conclusion” and they should be written in 10 font size, justify, bold and capital letters.

2. SRTM DEM error sources

SRTM DEM error sources can be abstracted to the baseline roll, phase, beam differential, timing, and position of the platform [2]. Figure 1 shows the SERTM error sources in abstracted form. The errors in interferometric measurements can be divided into two types: static and dynamic (time-varying) errors. The static errors were constant over the data collection period.

Because of their behavior, they can be calibrated using GCPs. Dynamic errors result from the motion of the interferometric mast and changes in the beam steering. Owing to their nature, dynamic errors can be partially waged by dynamic calibration and mosaicking. The SRTM error sources can be explained as follows. Baseline Roll Errors: These errors are caused by a lack of knowledge of the baseline roll angle, which induces a cross-track slope error in the proposed topography; therefore, its magnitude is equal to the roll error. Phase Errors: These errors are caused by both thermal or differential speckle noise and systematic phase changes owing to antenna pattern mismatches of the instrument electronics. Beam Differential Errors: Systematic phase differences between the SRTM beams induce height differences at beam overlaps. This difference can be time dynamic because the beam steering angles vary according to the topography to maintain the swath constant. Timing and Position Errors: These are caused by uncompensated delays in the system or errors in the estimated baseline position, resulting in geolocation errors. These errors were treated using targets with known positions that can be identified in the radar image or topography. Figure 2 shows the SRTM Measurement Geometry used to emphasize the nature and behavior of the interferometric data acquisition system.

To clarify the source of errors in SRTM data, one needs to understand the geometry of the interferometric measurement and attitude and orbit determination avionics (AODA). The main measurement vectors are B, the vector of the interferometric baseline; P, the vector from the origin of the WGS84-fixed origin to the phase center of the inboard antenna; V, the platform velocity vector; PG, the vector from the WGS84-fixed origin to the GPS antenna in the outboard frame; G, the vector from the outboard origin to the GPS antenna; Po, the vector from the outboard origin to the outboard phase center GPS antenna; A, the vector from the inboard origin to the outboard origin; and Pi, the vector from the inboard origin to the phase center of the inboard. The interferometric baseline B and the position of the inboard antenna phase center P can be determined by Equation 1-2.

$$B = A - P_i + P_o \quad (1)$$

$$P = P_G - (G + A - P_i) \quad (2)$$

Where:

A: the vector measured from the origin of the inboard system to the origin of the outboard system.

P_i: the vector measured from the origin of the inboard system to the phase center of the inboard antenna.

P_o: the vector measured from the origin of the outboard system to the phase center of the outboard antenna.

P_G: the vector measured from the Earth-fixed frame to a GPS receiver in the outboard antenna.

G: the vector measured from the origin of the outboard system to the GPS receiver.

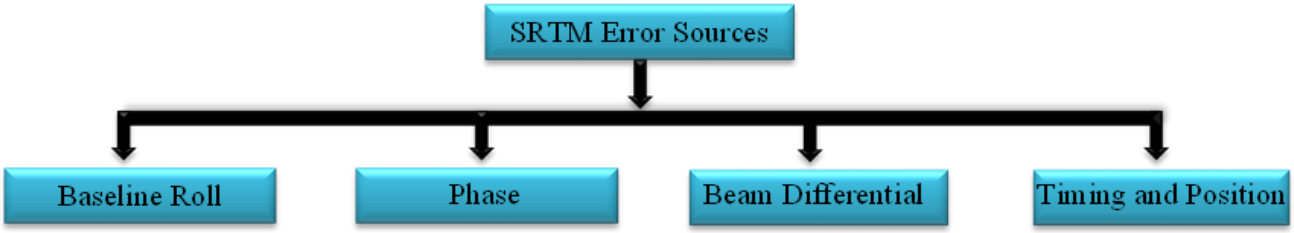

Figure 1. SRTM error sources.

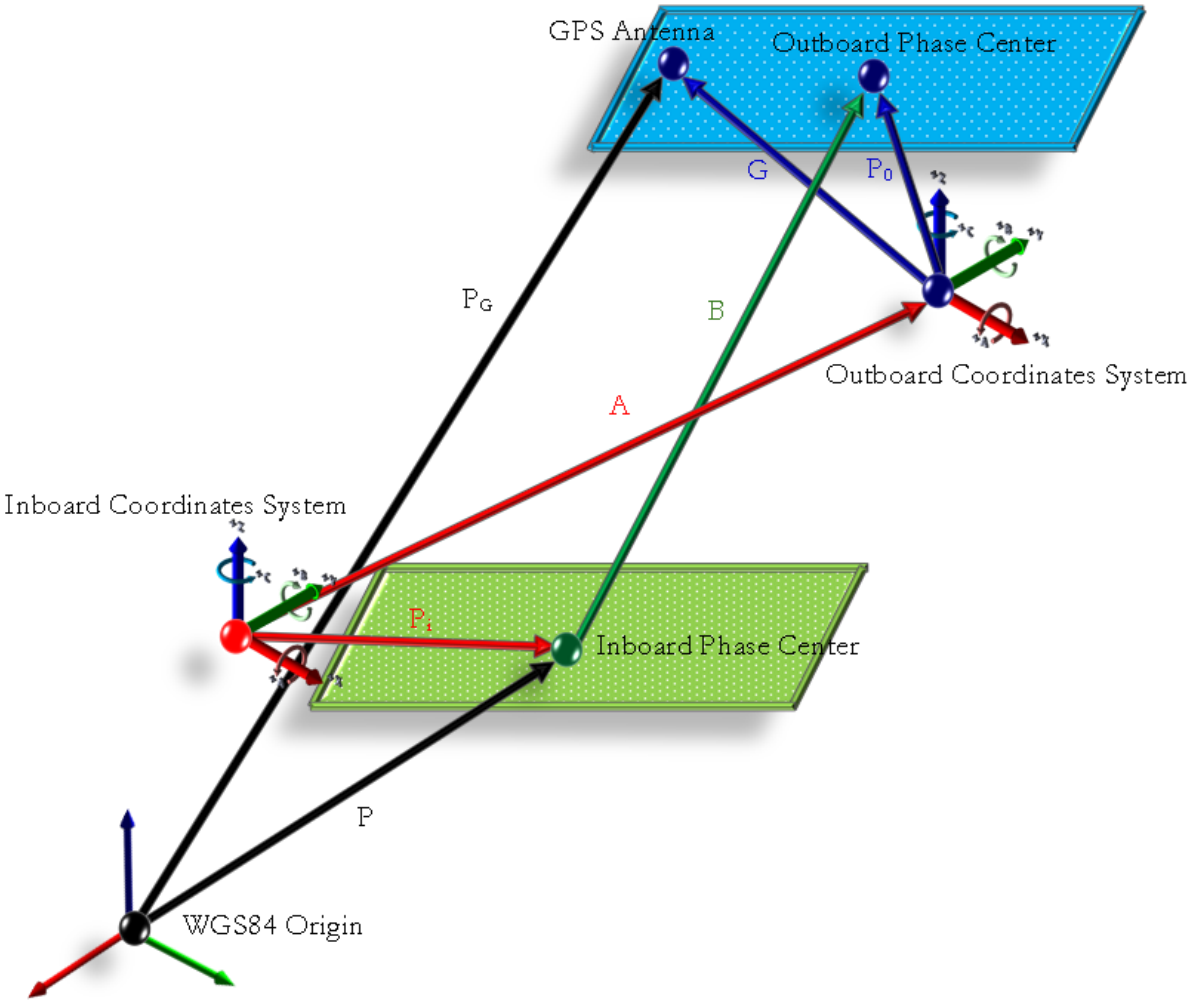

Figure 2. SRTM measurement geometry.

The error propagation of the interferometry can be deduced from the two Equations (1 and 2). Each error source has its own behavior and effect on the overall accuracy of the final DEM. Therefore, each error source had its own correction formulation. This study proposes an agglomerative methodology to express all error sources and their correction by applying a DANN in its supervised form. SRTM DEM correction can be carried out using many approaches, according to the literature. The most common general approach is mentioned in the previous section.

3. Method

This research is a trial to achieve a better representation of the SRTM DEM by applying registration using DANN. The methodology depends on using well-defined ground control points (GCPs) as a target for the DANN. While the SRTM DEM points are the input to the DANN, optimization can be carried out to achieve an output near the target GCPs. A selected group of points was chosen in both the SRTM DEM and the output DEM to verify the registration performance. Software is used to perform the tasks necessary to achieve the research objective. ENVI (by L3HARRIS) and DANNDO, which were developed by Serwa in [22, 23] are used to apply the necessary tasks in the developed system. A detailed description of the developed system is presented in the next section.

3.1. System overview

Figure 3 shows a systematic diagram of the proposed system. The system starts with the input of both the original SRTM DEM and a group of well-defined GPS points (GCPs) in the ENVI environment. Then, ENVI is used to perform the primitive task of determining the coordinates of the GCPs in the original SRTM DEM. At this stage, the GCPs have two coordinate values: the first belongs to the original SRTM DEM reference, while the second belongs to the GPS reference. Theoretically, both systems have the same reference in datum and projection (WGS 84), but practically, they are not the same because of the difference in conditions and data acquisition methodology. SRTM DEM depends on multiple sources such as KGPS distributed in large areas in addition to GEO-SAR and Ocean GCPs stations. The user depends directly on GPS in engineering applications. DANNDO software was then used to apply the DANN algorithm developed and refined by Serwa [10]. The result of this stage is the DANN SRTM DEM coordinates, which should be compared with the GPS reference

coordinates to adopt the accuracy assessment. To stand on a heavy base, other coordinates were obtained using the SRTM polynomials (first order) by assigning GPS coordinates as a destination (target) and SRTM DEM coordinates as the source (input). Therefore, a tri-tier comparison was adopted.

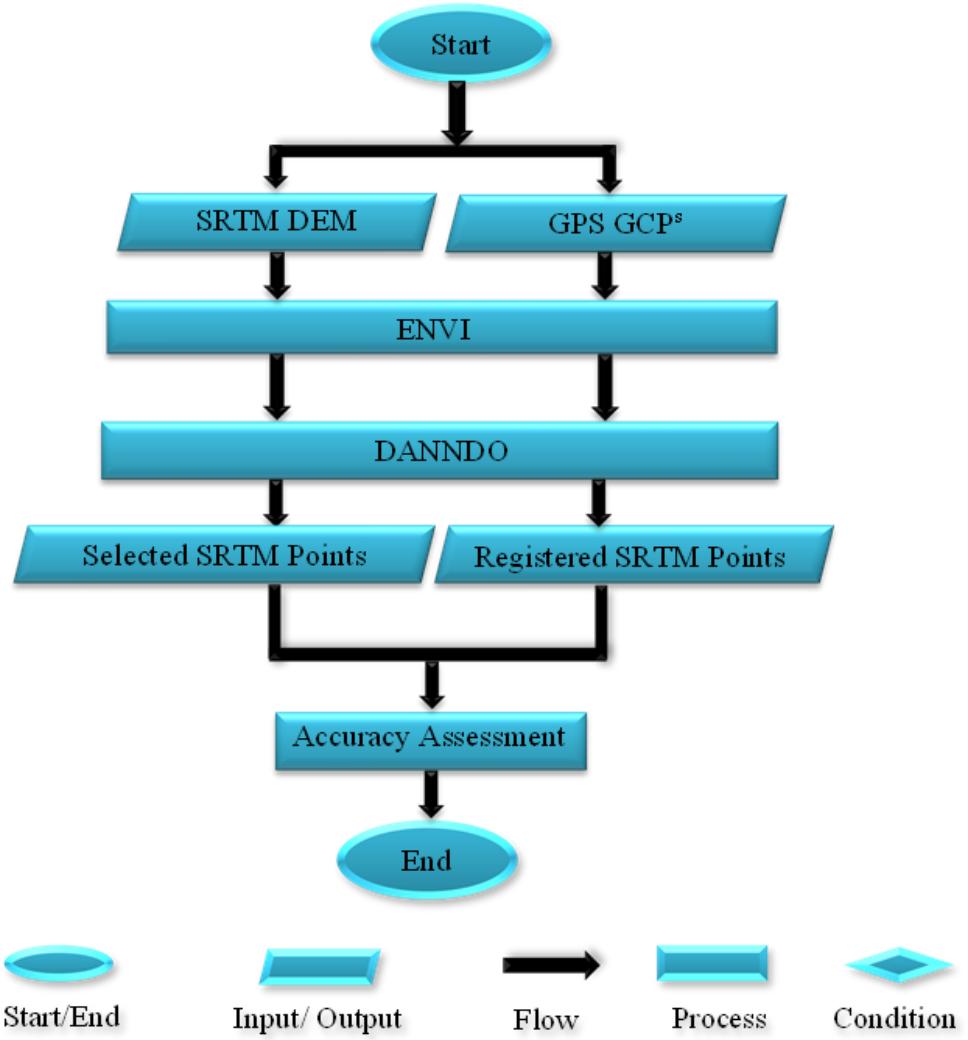

Figure 3. Systematic diagram of the research work.

3.2. Research data

The study area is part of the Aswan government in southern Egypt. SRTM DEM data of the research area were selected as the main data. Figure 4 shows the research area with the SRTM coverage. Four SRTM parts were required to cover the study area, so a mosaic was created. Eleven GCPs were selected for the study area, as shown in Figure 5. Ten virtual lines were used from each point to verify the linear accuracy of the registration process.

It is known that all requirements to obtain high measuring accuracy are taken such GCPs position selection, suitable measuring time 3–5 h, clear weather, etc. The selection of the GDOP in the GPS unit settings is necessary to obtain good accuracy even if there are more satellites.

Post-processing was performed to guarantee high accuracy. The distribution of GCPs is uniform and well defined. The measured coordinates of the 11 GCPs on the SRTM DEM model are tabulated in Table 1.

Each of the two GCPs is connected to form a virtual line, so we have fifty-five virtual lines (10+9+8+7+6+5+4+3+2+1). The tested fifty-five lines (L1 to L55) are tabulated as the first and second points in Table 2. The 1st refers to the starting point of the line and 2nd refers to the end point of the line. All the fifty-five lines were required to examine the distortion of the SRTM DEM as relative positioning. The coordinates of the 11 points were used to examine the distortion as absolute positioning. Both coordinates and lines were used to measure the performance level of the developed registration method. The values (coordinates and lengths) obtained from the GPS RTK devices were compared to the corresponding values obtained from the SRTM DEM (before and after registration). The values obtained from the GPS RTK were considered as the reference for this study. One must note that the tested lines varied in length to guarantee the generality of the study. The lines are used to express the relative accuracy of the selected GCPs and to examine the possible distortion of the registration process that may happen.

Figure 4. Study area with SRTM coverage.

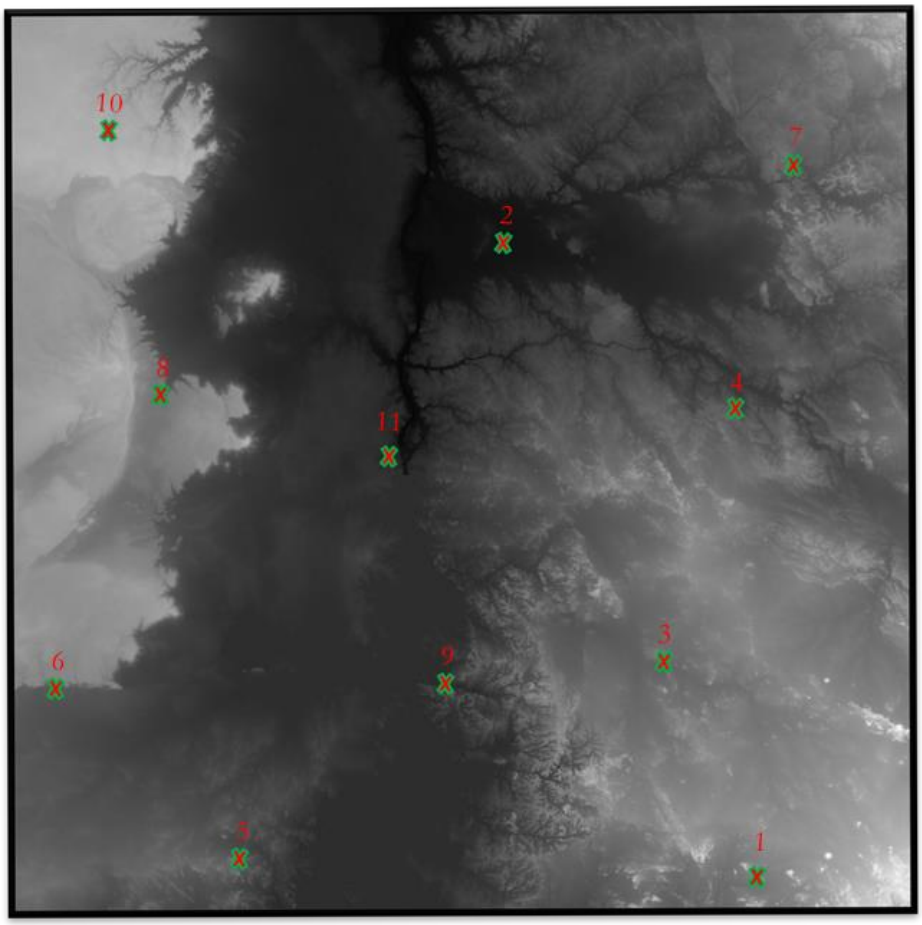

Figure 5. Distribution of GCPs in the study area.

Table 1. Coordinates of the GPS RTK coordinates of GCPs.

Pt #	X(m)	Y(m)	Z(m)
1	4894706.557	3225058.685	2506843.692
2	4873970.238	3179726.309	2602051.813
3	4889028.873	3203812.701	2544410.157
4	4876272.598	3184869.959	2591490.078
5	4932975.348	3167873.758	2504372.125
6	4936967.961	3139491.269	2531845.863
7	4844461.177	3174284.116	2662790.544
8	4924124.074	3118209.851	2582091.044
9	4923969.782	3149010.829	2544998.351
10	4892962.537	3124899.017	2632605.538
11	4896745.246	3164032.431	2578557.316

Table 2. List of the tested 55 lines.

Start / End	1	2	3	4	5	6	7	8	9	10	11
1	NA	L1	L2	L3	L4	L5	L6	L7	L8	L9	L10
2	NA	NA	L11	L12	L13	L14	L15	L16	L17	L18	L19
3	NA	NA	NA	L20	L21	L22	L23	L24	L25	L26	L27
4	NA	NA	NA	NA	L28	L29	L30	L31	L32	L33	L34
5	NA	NA	NA	NA	NA	L35	L36	L37	L38	L39	L40
6	NA	NA	NA	NA	NA	NA	L41	L42	L43	L44	L45
7	NA	NA	NA	NA	NA	NA	NA	L46	L47	L48	L49
8	NA	NA	NA	NA	NA	NA	NA	NA	L50	L51	L52
9	NA	NA	NA	NA	NA	NA	NA	NA	NA	L53	L54
10	NA	NA	NA	NA	NA	NA	NA	NA	NA	NA	L55
11	NA	NA	NA	NA	NA	NA	NA	NA	NA	NA	NA

3.3 DANN algorithm

In this study, DANN is adopted in the architecture of a multilayer perceptron (MLP), which is famous for such applications, and the algorithm of back propagation neural networks (BPNN) is adopted. The final presented algorithm is known as the DANN. The DANNDO software package of DANNDO is used to apply the required algorithms. One must be stabilized to declare any debate concerning the optimization process. The architecture of the DANN consists of an input layer (q) which represents the inputs, hidden layers (t, k, etc.) that represent the processing points of the input data and responsible for delivering the final processing to the output layer, and an output layer (m) which is responsible for producing the final network output, as indicated in Figure 6. In first (learning stage), the input vector Xq is the raw SRTM DEM point. The output vector Om is the corresponding computed value of the network. The structure of the DANN was selected after many trials to achieve a stable structure.

The DANN with BPNN was described by Serwa and Saleh [1].

The process of deep BPNN for remote sensing classification problems can be explained in the following steps:

Step 1: Input SRTM DEM coordinates.

Step 2: Input GPS coordinates for the selected GCPs.

Step 3: setting up training and testing data sets.

Step 4: Input SRTM DEM data vector to the input unit in the input layer.

Step 5: Get the output value of each neuron in the input layer.

Step 6: Get the input value for each neuron in the first hidden layer.

Step 7: Get the output value for each neuron in the first hidden layer.

Step 8: Get the input value for each neuron in the next hidden layer.

Step 9: Get the output value for each neuron in the current hidden layer.

Step 10: Repeat step 8 and Step 9 for all hidden layers.

Step11: Get the input value for each neuron in the output layer (the final output).

Step 12: Get the network error value using.

Step 13: Investigate if the error limit is exceeded or all pixels is entered go to step 22 otherwise continue.

Step 14: Get the error value in the output unit using.

Step 15: Update the weights between the output layer and the final hidden layer.

Step 16: Get the error in the hidden unit.

Step 17: Update the weights between the last hidden layer and the previous one.

Step 18: Repeat Step 16 and 17 for all intermediate hidden layers.

Step 19: Compute the error value in the first hidden layer neuron.

Step 20: Update the weights between the input layer and the first hidden layer.

Step 21: Go to step 4.

Step 22: Store the final weights.

Step 23: Apply steps 4 to 11 for all SRTM DEM data except training dataset.

Detailed information regarding the DANN algorithm is available in Serwa [10]. Figure 7 shows the main interface of DANNDO SW, which was used to apply the DANN with the BPNN algorithm. The tested network structure was 3,7,8 and 3 for the input, hidden, and output layers, respectively.

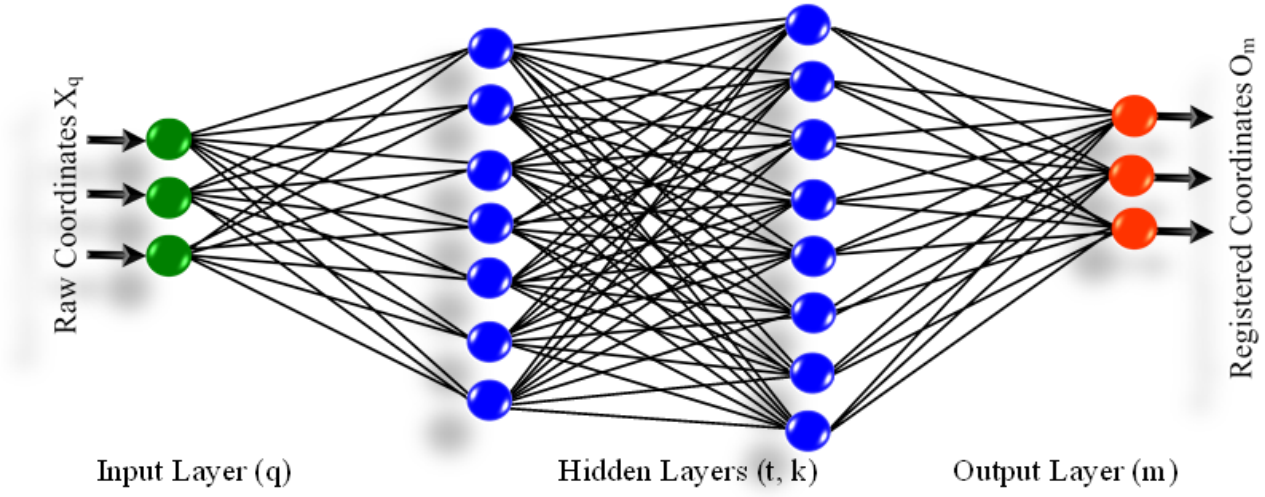

Figure 6. DANN architecture -input layer (q), hidden layers (t and k) and output layer (m).

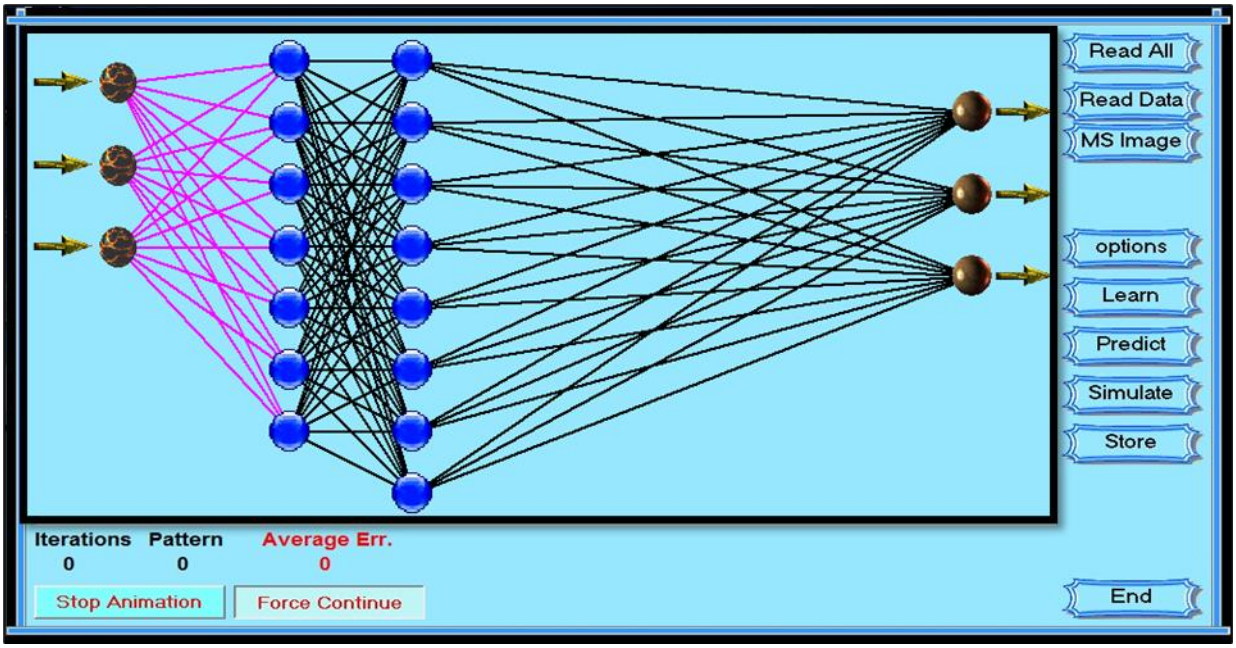

Figure 7. DANNDO SW interface.

4. Results

After the DANN is stabilized, it can be used to obtain the final output of the SRTM DEM coordinates. Table 3 shows the final errors in both DANN and SRTM DEM polynomials (1st order). While Table 4 lists the coordinates of the GCPs obtained from the GPS RTK Trimble device with the corresponding DANN SRTM DEM coordinates in addition to the SRTM DEM polynomials (1st order). GCPs have high precision (*.###) and it reaches mms. The coordinates of the GCPs were obtained by following the necessary requirements for using the GPS RTK device.

The SRTM DEM coordinates of the selected GCPs were obtained by registration using the DANN on DANNDO SW. The SRTM DEM polynomials was obtained by calculation using the solver in Excel. The SRTM DEM coordinates are the inputs for the DANN algorithm, whereas the GPS RTK coordinates are the target for the network output.

The results are summarized in Tables 4 and 5, for the X direction, σ_x= 21.990m with an average absolute error of 16.631m. For the Y direction, σ_y= 18.168m with an average absolute error of 14.129m. For the Z direction, σ_z= 28.707m with an average absolute error of 21.662m. For R, the space vector σ_R= 40.469m with an average absolute error of 34.217m.

Table 3. Coordinates of DANN SRTM DEM and SRTM DEM polynomials.

Point #	Errors in DANN Coordinates			Errors in Polynomials Coordinates		
	X(m)	Y(m)	Z(m)	X(m)	Y(m)	Z(m)
1	-46.302	-38.720	-8.997	-13.306	-32.120	11.511
2	-22.533	-3.023	2.251	-9.457	5.508	-10.419
3	8.767	-10.372	-67.198	35.043	-3.938	-58.323
4	-5.360	-11.895	22.904	9.907	-3.557	13.893
5	-3.475	-19.319	-63.205	48.841	-28.197	-17.804
6	-54.784	4.291	-60.991	-3.243	-8.099	-18.807
7	-2.109	-27.894	34.791	-9.58	-11.753	-9.088
8	-23.515	-8.025	-27.431	16.611	-18.664	-3.912
9	-52.207	-10.607	-19.145	-8.486	-18.567	11.982
10	-6.420	24.096	-40.972	13.15	22.655	-47.83
11	-42.056	1.470	28.011	-15.315	2.3696	34.720

Table 4. Coordinates of the GCPs in both GPS RTK, DANN SRTM DEM and SRTM DEM polynomials.

Point #	GPS RTK			DANN SRTM DEM			SRTM DEM Polynomials		
	X(m)	Y(m)	Z(m)	X(m)	Y(m)	Z(m)	X(m)	Y(m)	Z(m)
1	4894706.557	3225058.685	2506843.692	4894719.864	3225090.806	2506832.181	4894752.86	3225097.405	2506852.689
2	4873970.238	3179726.309	2602051.813	4873979.695	3179720.801	2602062.232	4873992.771	3179729.332	2602049.561
3	4889028.873	3203812.701	2544410.157	4888993.83	3203816.64	2544468.48	4889020.105	3203823.073	2544477.356
4	4876272.598	3184869.959	2591490.078	4876262.691	3184873.516	2591476.185	4876277.958	3184881.855	2591467.173
5	4932975.348	3167873.758	2504372.125	4932926.507	3167901.956	2504389.93	4932978.824	3167893.077	2504435.331
6	4936967.961	3139491.269	2531845.863	4936971.205	3139499.368	2531864.671	4937022.745	3139486.977	2531906.854
7	4844461.177	3174284.116	2662790.544	4844470.757	3174295.869	2662799.632	4844463.287	3174312.01	2662755.753
8	4924124.074	3118209.851	2582091.044	4924107.463	3118228.515	2582094.956	4924147.589	3118217.877	2582118.475
9	4923969.782	3149010.829	2544998.351	4923978.268	3149029.396	2544986.369	4924021.989	3149021.436	2545017.497
10	4892962.537	3124899.017	2632605.538	4892949.387	3124876.362	2632653.368	4892968.958	3124874.92	2632646.51
11	4896745.246	3164032.431	2578557.316	4896760.561	3164030.061	2578522.595	4896787.302	3164030.96	2578529.304

Table 5. Results summary.

	σ_x(m)	dX Avg(m)	σ_y(m)	dY Avg(m)	σ_z(m)	dZ Avg(m)	σ_R(m)	dR Avg(m)
DANN SRTM DEM	21.990	16.631	18.168	14.129	28.707	21.662	40.469	34.217
SRTM DEM Polynomials	32.959	24.321	19.201	14.519	41.992	34.172	56.731	51.259

X, Y, Z, and R express the absolute positioning of the space coordinates. The results for the lengths (relative positioning) for all 55 lines are σ_L = 37.263m with an average absolute error of 30.032m. For the SRTM polynomials, σ_x=22.763m (not better than DANN) with average absolute error =24.321m, σ_y=19.201m (worse than DANN) with average absolute error= 14.519m, σ_z=41.992m (better than DANN) with average absolute error=34.172m, and σ_R=56.731m (worse than DANN) with average absolute error=51.259m. A 2¬nd order polynomials is applied but it gives a worst result. To determine the potential of the DANN registration methodology, a statistical test of hypothesis was conducted. The performance of the DANN registration can be measured in many ways. The most significant method was to test the hypothesis. Assuming a 95% level of confidence, the first hypothesis is that there is no significant difference between the true (reference) GPS RTK measurements and the resulting DANN-registered measurements, which indicates success. The alternative is that there is a significant difference between them, which indicates failure of the DANN registration process. The testing sample is 11 in the case of X, Y, Z, and R (absolute position) < 30, so that the degree of freedom for is 10 for both hypotheses. Using a 95% level of significance, a critical value of ±2σ can be obtained as the acceptance limit for all measurements. It is obvious that all average absolute error values for all measurements are less than 2σ or even less than σ (68% level of significance). Therefore, we must accept the hypothesis that there is no significant difference between GPS RTK measurements and DANN-registered measurements. The alternative hypothesis must be rejected, and registration using DANN is reliable. Figure 8 shows the final registered SRTM DEM with GCPs.

5. Conclusion

The results show that using DANN is feasible due to the enhancement in accuracy compared with the classical napping polynomials. Referring to the research objective, it can be concluded that using the DANN registration methodology is the most effective. The reason behind the effectiveness is obtaining a good (small) acceptable distortion in both absolute positioning (X, Y, Z, and R) and relative positioning (lengths). It should be noted that there is no need to compare the research results with any other registration method because of the dependence on high-accuracy GPS-RTK GCPs. In other words, the ground reference is very accurate, and the DANN registration results show no significant difference. Although the DANN algorithm is very sensitive to the initial network weights, it provides good results in this research because of the use of a high-accuracy network target (GPS RTK GCPs). Accordingly, it is recommended to use the DANN registration methodology with high-accuracy GPS-RTK GCPs. When using a first-order polynomials to register the SRTM DEM, it is obvious that it is not better at all because most errors in all directions are higher than DANN method. Even applying 2nd order polynomials, it is

not better than DANN. One important note concerning the limitations of this study is that it can be considered as a local system for a certain part of the earth's surface. The reason is the errors and distortions that are dependent on the size of the area may increase. The behavior in such a case cannot be predicted.

For future recommendations, one should consider using deep learning algorithms (e.g. convolution neural networks, deep belief neural networks etc.).

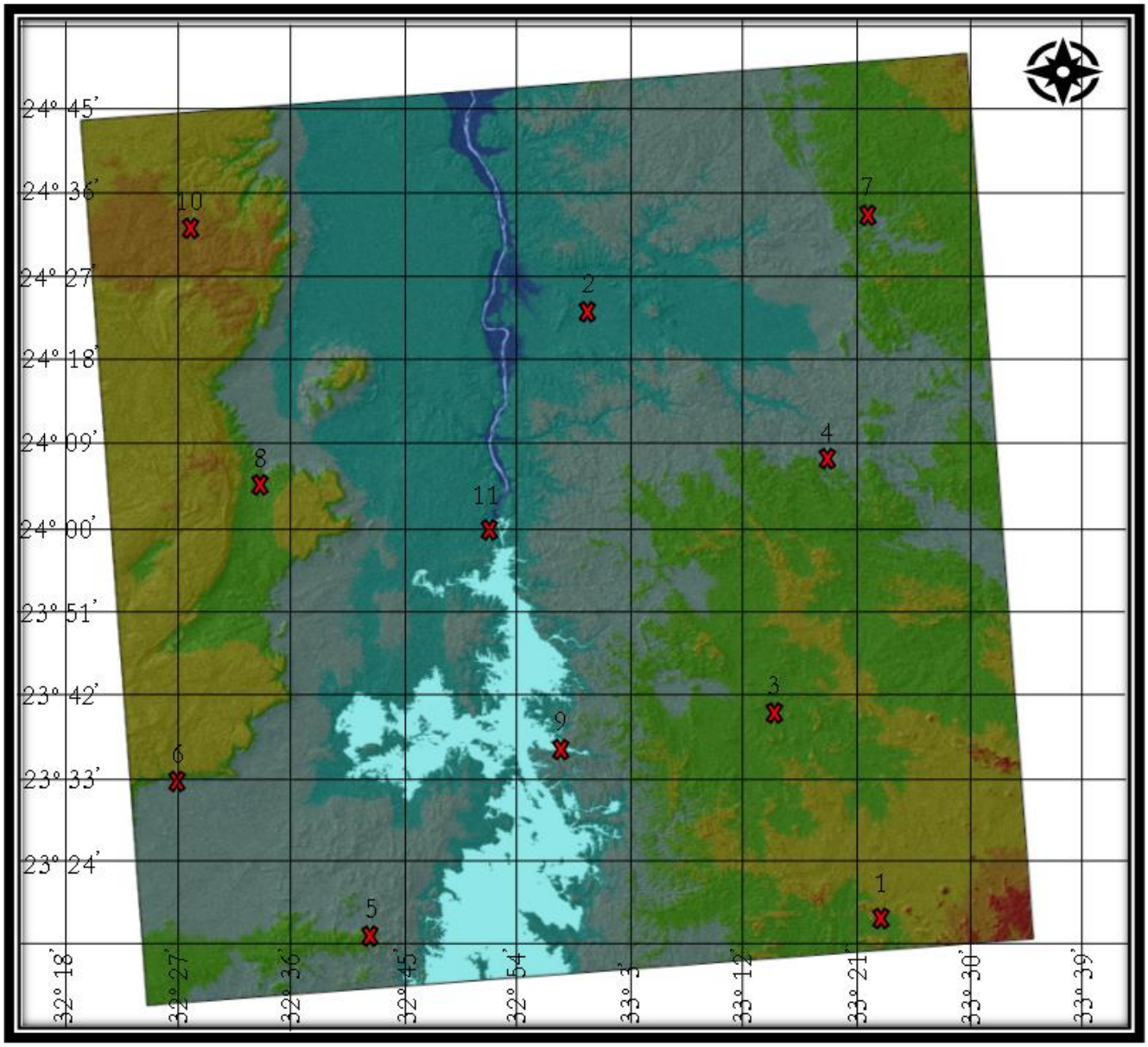

Figure 8. The final registered DEM with GCPs shown.

Author contributions

Ahmed Serwa: Conceptualization, Methodology, Software, Field study and Writing-Original draft preparation

Abdul Baser Qasimi: Data curation, Writing-Original draft preparation, Software, Validation.

Vahid Isazade: Visualization, Investigation, Writing-Reviewing and Editing.

Conflicts of interest

The authors declare no conflicts of interest.

References

1. Serwa, A., & Saleh, M. (2021). New semi-automatic 3D registration method for terrestrial laser scanning data of bridge structures based on artificial neural networks. The Egyptian Journal of Remote Sensing and Space Science, 24(3), 787-798. https://doi.org/10.1016/j.ejrs.2021.06.003
2. Rodriguez, E., Morris, C. S., Belz, J. E., Chapin, E. C., Martin, J. M., Daffer, W., & Hensley, S. (2005). An assessment of the SRTM topographic products.
3. Chen, C., Yang, S., & Li, Y. (2020). Accuracy assessment and correction of SRTM DEM using ICESat/GLAS data under data coregistration. Remote Sensing, 12(20), 3435. https://doi.org/10.3390/rs12203435

4. Su, Y., & Guo, Q. (2014). A practical method for SRTM DEM correction over vegetated mountain areas. ISPRS Journal of Photogrammetry and Remote Sensing, 87, 216-228. https://doi.org/10.1016/j.isprsjprs.2013.11.009
5. Su, Y., Guo, Q., Ma, Q., & Li, W. (2015). SRTM DEM correction in vegetated mountain areas through the integration of spaceborne LiDAR, airborne LiDAR, and optical imagery. Remote Sensing, 7(9), 11202-11225. https://doi.org/10.3390/rs70911202
6. Ochoa, C. G., Vives, L., Zimmermann, E., Masson, I., Fajardo, L., & Scioli, C. (2019). Analysis and correction of digital elevation models for plain areas. Photogrammetric Engineering & Remote Sensing, 85(3), 209-219. https://doi.org/10.14358/PERS.85.3.209
7. Zhou, C., Zhang, G., Yang, Z., Ao, M., Liu, Z., & Zhu, J. (2020). An adaptive terrain-dependent method for SRTM DEM correction over mountainous areas. IEEE Access, 8, 130878-130887. https://doi.org/10.1109/ACCESS.2020.3009851
8. Julzarika, A., Harintaka, H., & Kartika, T. (2021). Vegetation Height Estimation using Satellite Remote Sensing in Peat Land of Central Kalimantan. Journal of Environmental Analysis and Progress, 6(1), 24-34. https://doi.org/10.24221/jeap.6.1.2021.3001.024-034
9. Serwa, A., & El-Semary, H. H. (2020). Semi-automatic general approach to achieve the practical number of clusters for classification of remote sensing MS satellite images. Spatial Information Research, 28(2), 203-213. https://doi.org/10.1007/s41324-019-00283-z
10. Serwa, A. (2022). Development of soft computational simulator for optimized deep artificial neural networks for geomatics applications: remote sensing classification as an application. Geodesy and Cartography, 48(4), 224-232. https://doi.org/10.3846/gac.2022.15642
11. Altunel, A. O. (2023). The effect of DEM resolution on topographic wetness index calculation and visualization: An insight to the hidden danger unraveled in Bozkurt in August, 2021. International Journal of Engineering and Geosciences, 8(2), 165-172. https://doi.org/10.26833/ijeg.1110560
12. Bildirici, İ. Ö., & Abbak, R. A. (2020). Türkiye ve çevresinde SRTM sayısal yükseklik modelinin doğruluğu. Geomatik, 5(1), 1-9. https://doi.org/10.29128/geomatik.551071
13. Çubukçu, E. A., Demir, V., & Sevimli, M. F. (2022). Digital elevation modeling using artificial neural networks, deterministic and geostatistical interpolation methods. Turkish Journal of Engineering, 6(3), 199-205. https://doi.org/10.31127/tuje.889570
14. Yakar, M. (2009). Digital elevation model generation by robotic total station instrument. Experimental Techniques, 33(2), 52-59. https://doi.org/10.1111/j.1747-1567.2008.00375.x
15. Yalçın, C. (2022). DEM and GIS-based assessment of structural elements in the collision zone: Çağlayancerit, Kahramanmaraş (Türkiye). Advanced Remote Sensing, 2(2), 66-73.
16. Yılmaz, A., & Erdoğan, M. (2018). Designing high resolution countrywide DEM for Turkey. International Journal of Engineering and Geosciences, 3(3), 98-107. https://doi.org/10.26833/ijeg.384822
17. Yakar, M., Yilmaz, H. M., & Yurt, K. (2010). The effect of grid resolution in defining terrain surface. Experimental Techniques, 34, 23-29. https://doi.org/10.1111/j.1747-1567.2009.00553.x
18. Sariturk, B., Bayram, B., Duran, Z., & Seker, D. Z. (2020). Feature extraction from satellite images using segnet and fully convolutional networks (FCN). International Journal of Engineering and Geosciences, 5(3), 138-143. https://doi.org/10.26833/ijeg.645426
19. Yakar, M., Yilmaz, H. M., & Mutluoglu, O. (2014). Performance of photogrammetric and terrestrial laser scanning methods in volume computing of excavtion and filling areas. Arabian Journal for Science and Engineering, 39, 387-394. https://doi.org/10.1007/s13369-013-0853-1
20. Browning Jr, D. C. (2024). Close-range photogrammetry for analysis of rock relief details: An investigation of symbols purported to be Jewish Menorahs in Rough Cilicia. Mersin Photogrammetry Journal, 6(1), 39-51. https://doi.org/10.53093/mephoj.1434605
21. Yilmaz, H. M., Yakar, M., Mutluoglu, O., Kavurmaci, M. M., & Yurt, K. (2012). Monitoring of soil erosion in Cappadocia region (Selime-Aksaray Turkey). Environmental Earth Sciences, 66, 75-81. https://doi.org/10.1007/s12665-011-1208-4
22. Serwa, A. (2017). Optimizing activation function in deep artificial neural networks approach for landcover fuzzy pixel-based classification. International Journal of Remote Sensing Applications, 7, 1-10. https://doi.org/10.14355/ijrsa.2017.07.001
23. Ismail, S. A., Serwa, A., Abood, A., Fayed, B., Ismail, S. A., & Hashem, A. M. (2019). A Study of the Use of Deep Artificial Neural Network in the Optimization of the Production of Antifungal Exochitinase Compared with the Response Surface Methodology. Jordan Journal of Biological Sciences, 12(5), 543-551.